ELSEVIER

Soil Dynamics and Earthquake Engineering 21 (2001) 259–271

SOIL DYNAMICS AND EARTHQUAKE ENGINEERING

www.elsevier.com/locate/soildyn

Seismic analysis of lock–soil–fluid systems by hybrid BEM–FEM

Chaojin Xu[a], C.C. Spyrakos[b,*]

[a]*Algor Inc., 150 Beta Drive, Pittsburgh, PA 15238, USA*

[b]*Department of Civil Engineering, Laboratory for Earthquake Engineering, National Technical University of Athens, Zografos, GR-15700, Athens, Greece*

Accepted 25 November 2000

Abstract

A study of soil–structure–fluid interaction (SSFI) of a lock system subjected to harmonic seismic excitation is presented. The water contained lock is embedded in layered soils supported by a half-space bedrock. The ground excitation is prescribed at the soil–bedrock interface. The response is numerically obtained through a hybrid boundary element (BEM) finite element method (FEM) formulation. The semi-infinite soil and the fluid are modeled by the BEM and the lock is modeled by the FEM. The equilibrium equation for the lock system is obtained by enforcing compatibility and equilibrium conditions at the fluid–structure, soil–structure and soil–layer interfaces under conditions of plane strain. To the authors' knowledge this is the first study of a lock system that considers the effects of dynamic soil–fluid–structure interaction through a BEM–FEM methodology. A numerical example and parametric studies are presented to examine the effects of the presence of water, lock stiffness, and lock embedment on the response. © 2001 Published by Elsevier Science Ltd.

Keywords: Seismic analysis; Boundary element method; Finite element method; Soil–structure–fluid interaction

1. Introduction

Seismic analysis of large systems considering soil–structure–fluid interaction (SSFI) result in a rather involved mathematical treatment when factors such as unbounded extent of soil and fluid, compressibility of water, geometry of structure, surface waves of water, and flexibility of structure, are taken into account. Systems that SSFI should be considered include: (1) submerged or off-shore; (2) dam–reservoir–soil; (3) storage tank; (4) intake towers; and (5) lock and dam. Chen [1] has given a review on the research up to 1982 of submerged off-shore systems. Developments on this topic can be found in Refs. [2,3]. A comprehensive review of the analysis of a dam–reservoir–soil system has been presented by Dominguez et al. [4]. Research covering different types of dam–soil–reservoir systems has been reported by Refs. [5–11].

In this study, the lock system is a fluid contained open-channel structure embedded in layered soil, see Fig. 1. It presents many similarities with a storage tank system, although the storage tank system is usually placed above the ground level and contains a bounded amount of fluid. A discussion on storage tank systems has been given by Antes and Latz [12]. In the early stage of studying the seismic response of storage tank systems, the tank was assumed to be rigid and anchored to a rigid base, e.g. Ref. [13]. Realizing that the flexibility of the tank can play an important role on the seismic response, later methods tried to address the issue. Representative semi-analytical procedures employ assumed modes and added masses to describe the displacement of the tank and account for the effect of the fluid–structure and SSFI. Representative works on the topic include Refs. [14–23]. A recent work [24] on the seismic response of towers and intake towers studies the effect of partial separation of the foundation from the soil and presents a review on pertinent topics including literature on the effects of soil–structure and SSFI.

As an alternative method, the finite element method (FEM) has found its application on the seismic analysis of storage tank systems. One of the primary advantages of FEM over semi-analytical procedures is that it is not limited to simple geometry structure. Edwards [25] is known to be the first to introduce FEM to SSFI. Other early studies are presented in Refs. [26–28]. In all these studies, the tank is assumed to be rigidly connected to the soil. A representative study [29] investigates the behavior of unanchored and flexible tanks.

A well documented disadvantage of FEM is its difficulty in modeling the semi-infinite soil and fluid domains. However, combination of the boundary element method (BEM) and FEM can overcome this difficulty. Although a large number of papers have been published on the

* Corresponding author. Tel.: +30-1-7721187; fax: +30-1-7721182.
E-mail address: chris@central.ntua.gr (C.C. Spyrakos).

0267-7261/01/$ - see front matter © 2001 Published by Elsevier Science Ltd.
PII: S0267-7261(00)00101-9

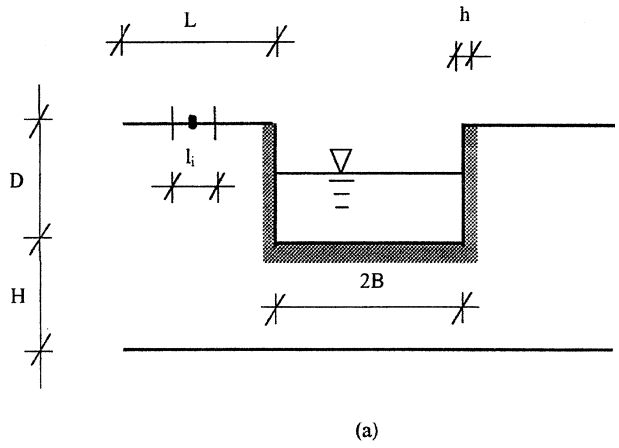

Fig. 1. Fluid contained lock on layered soil.

application of BEM or FEM/BEM on the seismic analysis of systems considering soil–structure interaction (SSI), very limited studies can be found in the literature, where issues of soil–structure–fluid interaction (SSFI) are addressed. Two early applications of BEM to structure–fluid interaction (SFI) of fluid contained tanks appeared in 1980. In these studies the tanks are modeled by FEM and the incompressible fluid domain by BEM [30,31]. Koh et al. [32] have studied the dynamic response of storage tanks by combining BEM with the FEM. In all these works, no soil–structure interaction is considered. Therefore, they can be more properly classified as structure–fluid interaction (SFI), not SSFI problems. To the authors' knowledge, one of the first investigations to include soil–structure–fluid interaction was Ref. [33]. In a paper by Antes and Latz [12], the SSFI is studied in the frequency domain by the so-called BEM–FIS method. In their work, the compressibility of fluid and surface sloshing is also included, and the SSFI is considered by attaching a flexible tank to a rigid foundation supported by an elastic soil.

The structural system studied in this work is a lock system supported by a layered soil, see Fig. 1. The SSFI is treated by a hybrid FEM/BEM in the frequency domain. Plate elements are employed to model the U-lock, and the BEM is applied to model the fluid domain and the layered soil. In deriving the system equations, the equilibrium and compatibility conditions at the fluid–structure, soil–structure, and the soil layer interfaces are used.

2. System description

The system consists of a fluid–contained structure embedded in layered soil deposits. Structures of this kind include hydraulic channels, locks, long storage tanks either open or covered by a flexible roof. One dimension of the structure is much longer than the other two with uniform loading so that the problem satisfies conditions of plane–strain, see Fig. 1. Also, the thickness of the walls is small compared to the width of the structure, which justifies application of thin plate theory. In order to consider the variation of soil properties along the depth, the half-space soil domain is divided into 'n' layers with different material properties. The system is subjected to harmonic seismic excitations described at the bedrock–soil layer interface.

The following sections describe the derivation of the equilibrium equation for each substructure, that is, the structure, the fluid, and the soil. The BEM is used to treat the soil and fluid domains, and the FEM is used to model the walls and bottom lining of the lock. Such an approach utilizes the advantages of each method. Specifically, BEM accounts for radiation damping automatically and restricts modeling of contact areas only, while the FEM is most suitable to model the finite size side and bottom walls of the lock [34].

The notation shown in Fig. 1 is adopted. The free surface of the fluid is denoted by 'a' and the structure–fluid interface is indicated by 'b'. The top soil (1) layer has boundaries 'e', 'c', and '1'. The boundary 'e' is the free surface, boundary 'c' is the soil–structure interface, and boundary '1' is the contact interface with layer (2). The bottom layer (n) has a top boundary '$n-1$' which is the contact interface with layer ($n-1$) and bottom boundary 'n' which represents the interface with the half-space where the seismic excitation prescribed. A general layer (k) between the top layer and the bottom layer has top boundary '$k-1$' and bottom boundary 'k', where '$k-1$' is the contact interface between layers ($k-1$) and (k).

3. BEM formulation and numerical treatment for the fluid and soil domains

3.1. BEM formulation for the fluid

For a compressible inviscid fluid with small displacements and zero initial conditions, the governing equation for the hydrodynamic pressure in excess of the hydrostatic pressure expressed in the frequency domain is the Helmholtz equation [35–37]:

$$\Delta^2 P(\vec{x},\omega) + \kappa^2 P(\vec{x},\omega) = 0 \tag{1}$$

where $P(\vec{x},\omega)$ is the frequency response function for hydrodynamic pressure, $\kappa = \omega/c$ is the wave number, c is the velocity of sound in the fluid, and ω is the circular frequency of the excitation.

The corresponding boundary conditions are

$$P(\vec{x},\omega) = p(\vec{x},\omega) \;\; x \in \Gamma_1 \tag{2}$$

$$Q(\vec{x},\omega) = q(\vec{x},\omega) \;\; x \in \Gamma_2$$

where Γ_1 is the free surface boundary, and Γ_2 is the

contact interface, low case parameters p and q represent known values at the boundaries, and Q is related to P as given by

$$Q = \frac{\partial P}{\partial \vec{n}} \tag{3}$$

in which $\vec{n}$ is the outward normal to the fluid boundary.

The numerical solution of Eq. (1) together with the boundary conditions is obtained by applying the BEM. The starting integral equation of BEM for the fluid in the frequency domain is given by [38]

$$\delta(\vec{\xi})P(\vec{\xi}) = \int_{\Gamma}[Q(\vec{x})P^*(\vec{x},\vec{\xi};\kappa) - P(\vec{x})Q^*(\vec{x},\vec{\xi};\kappa)]\mathrm{d}\Gamma \tag{4}$$

where $\delta(\vec{\xi})$ depends on the smoothness of boundaries, P^* is the fundamental solution of Eq. (1) which is given by

$$P(\vec{x},\vec{\xi},\kappa) = \frac{1}{2\pi}K_0(\mathrm{i}\kappa r) \tag{5}$$

Q^* is the derivative of P^* with respect to the outward normal, and $\vec{r}$ is the distance between vectors $\vec{x}$ and $\vec{\xi}$. Dividing the boundary into n elements and using constant boundary elements, see Fig. 2(a), a set of n linear equations can be obtained [36,37]

$$[H]\{P\} = [G]\{Q\} \tag{6}$$

where $\{H\}$, [G] are $n \times n$ matrices and $\{P\}$, $\{Q\}$ are vectors of length n. A simplified form of Eq. (6) is given by

$$[D]\{Q\} = \{P\} \tag{7}$$

where $[D] = [H]^{-1}[G]$.

The degrees-of-freedom at the free surface in Eq. (6) can be condensed by employing the boundary conditions at the free surface of the fluid. At the free surface, if the effect of the surface waves is neglected, the boundary condition is

$$\{P_\mathrm{b}\} = \{0\} \tag{8}$$

If the waves at the free surface are considered, then $\{P_\mathrm{a}\}$ is related to $\{Q_\mathrm{a}\}$ by [12]

$$\{P_\mathrm{a}) = \frac{g}{\omega^2}\{Q_\mathrm{a}\} \tag{9}$$

where g is the acceleration of gravity.

Eq. (7) can be rewritten for the boundaries 'a' and 'b' as [37]

$$\begin{bmatrix} D_{\mathrm{aa}} & D_{\mathrm{ab}} \\ D_{\mathrm{ba}} & D_{\mathrm{bb}} \end{bmatrix}\begin{Bmatrix} Q_\mathrm{a} \\ Q_\mathrm{b} \end{Bmatrix} = \begin{Bmatrix} P_\mathrm{a} \\ P_\mathrm{b} \end{Bmatrix} \tag{10}$$

Substitution of the boundary condition of Eq. (9) into Eq. (10) yields

$$\begin{bmatrix} D_{\mathrm{aa}} - \frac{g}{\omega^2}I_{\mathrm{aa}} & D_{\mathrm{ab}} \\ D_{\mathrm{ba}} & D_{\mathrm{bb}} \end{bmatrix}\begin{Bmatrix} Q_\mathrm{a} \\ Q_\mathrm{b} \end{Bmatrix} = \begin{Bmatrix} 0 \\ P_\mathrm{b} \end{Bmatrix} \tag{11}$$

From the first half of Eq. (11), $\{Q_\mathrm{a}\}$ is related to $\{Q_\mathrm{b}\}$ as given by

$$\{Q_\mathrm{a}\} = -\left[[D_{\mathrm{aa}}] - \frac{g}{\omega^2}I_{\mathrm{aa}}\right]^{-1}[D_{\mathrm{ab}}]\{D_\mathrm{b}\} \tag{12}$$

Substitution of the expression for $\{Q_\mathrm{b}\}$ into the second half of Eq. (11) yields a condensed equation expressed in $\{P_\mathrm{b}\}$ and $\{Q_\mathrm{b}\}$ at the structure–fluid contact interface only, that is

$$[D']\{Q_\mathrm{b}\} = \{P_\mathrm{b}\} \tag{13}$$

where

$$[D'] = [D_{\mathrm{bb}}] - [D_{\mathrm{ba}}]\left[[D_{\mathrm{aa}}] - \frac{g}{\omega^2}I_{\mathrm{aa}}\right]^{-1}[D_{\mathrm{ab}}] \tag{14}$$

In order to relate the variables$\{P_\mathrm{b}\}$ and $\{Q_\mathrm{b}\}$ of the fluid to the equilibrium equations for the soil and structure, that are expressed in terms of nodal forces and nodal displacements, use must be made of the boundary conditions at the structure–fluid contact interface, that is

$$q(\vec{x},t) = \rho\ddot{u}_i(\vec{x},t)_{n_i}(\vec{x},t) \tag{15}$$

and

$$\begin{Bmatrix} t_x^i(\vec{x},t) \\ t_y^i(\vec{x},t) \end{Bmatrix} = p^i(\vec{x},t)\begin{Bmatrix} n_x^i \\ n_y^i \end{Bmatrix} \tag{16}$$

where t_x^i, t_y^i are the components of the traction at the ith element, and n_x^i, n_y^i are the corresponding outwards normals [37], and $\ddot{u}_i$ is the absolute acceleration of the structure.

From the boundary condition expressed by Eq. (15), $\{Q_\mathrm{b}\}$ is related to $\{U_\mathrm{b}\}$ in the frequency domain as given by

$$\{Q_\mathrm{b}\} = \rho_\mathrm{s}\alpha\omega^2[C_\mathrm{b}]\{U_\mathrm{b}\} \tag{17}$$

where

$$[C_\mathrm{b}] = \begin{Bmatrix} n_x^1, n_y^1 & & & \\ & n_x^2, n_y^2 & & \\ & & \cdots & \\ & & & n_x^m, n_y^m \end{Bmatrix} \tag{18}$$

in which $m$denotes the total number of boundary elements at the structure–fluid contact area.

Similarly, based on the coupling condition of Eq. (16), $\{P_\mathrm{b}\}$ is related to $\{T_\mathrm{b}\}$ by

$$\{T_\mathrm{b}\} - [C_\mathrm{b}]^\mathrm{T}\{P_\mathrm{b}\} \tag{19}$$

where

$$\{T_\mathrm{b}\} = (T_x^1, T_y^1, T_x^2, T_y^2, \ldots, T_x^m, T_y^m\}^\mathrm{T} \tag{20}$$

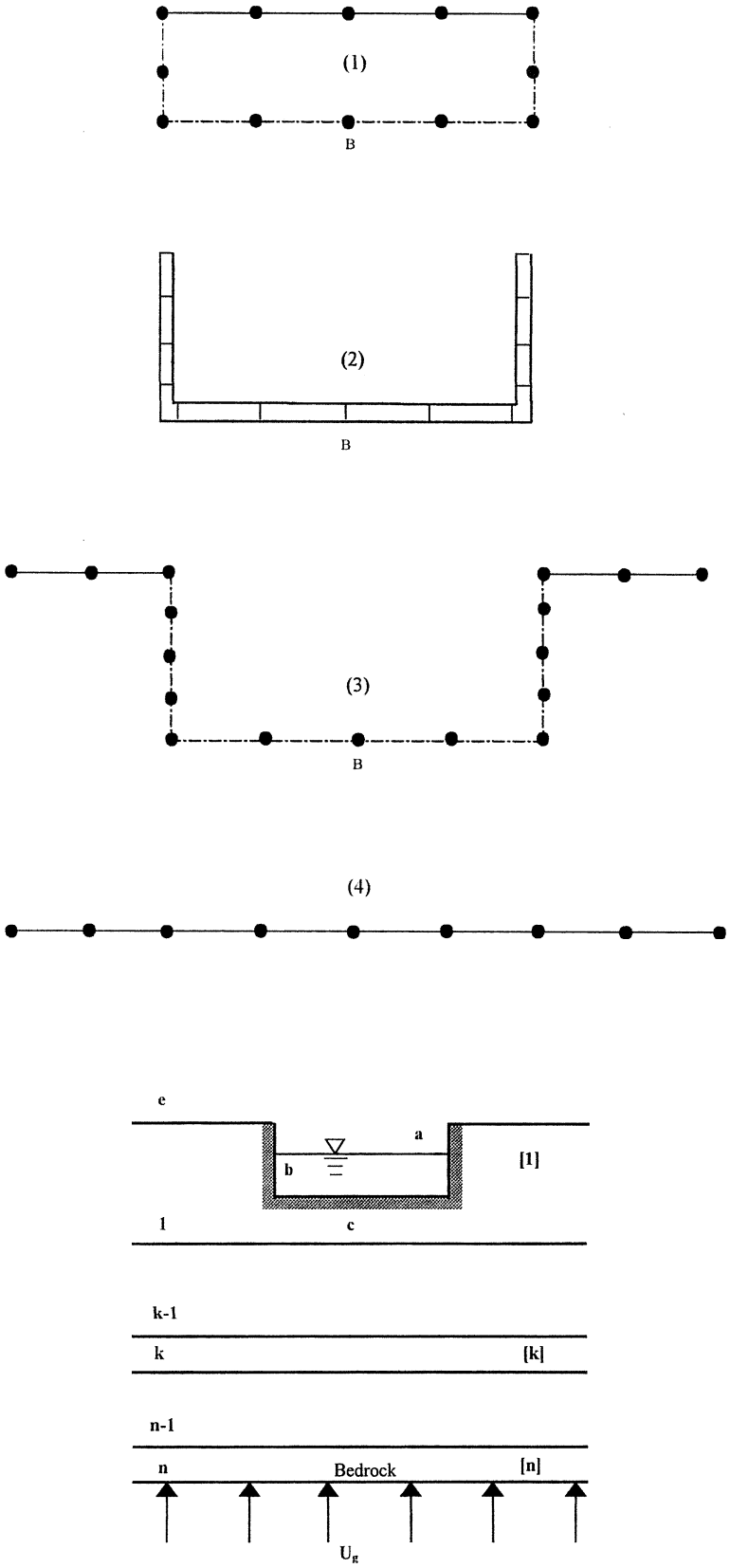

Fig. 2. (a) Discretization of the lock–soil–fluid system: (1) fluid; (2) lock-lining; (3) soil interface; and (4) soil–bedrock interface. (b) Geometry of lock–soil–fluid system.

and

$$\{P_b\} = \{P_x^1, P_y^1, P_x^2, P_y^2, ..., P_x^m, P_y^m\}^T \tag{21}$$

Also, the nodal force vector $\{F_b\}$ is related to the tractions as given by

$$\{F_b\} = [L_b]\{T_b\} \tag{22}$$

where

$$\{F_b\} = \{F_x^1, F_y^1, F_x^2, F_y^2, ..., F_x^m, F_y^m\}^T \tag{23}$$

and

$$[L_b] = \begin{Bmatrix} l_1 & 0 & ... & ... & ... & 0 \\ 0 & l_2 & ... & ... & ... & 0 \\ ... & ... & ... & ... & ... & ... \\ 0 & 0 & ... & ... & ... & l_m \end{Bmatrix} \tag{24}$$

in which l_i is the length of the ith boundary element.

In view of Eq. (19), Eq. (22) can be expressed as

$$\{F_b\} = [L_b][C_b]^T\{P_b\} \tag{25}$$

Substituting the expression for $\{Q_b\}$ from Eq. (17) into Eq. (13) and multiplying both sides of the resulting equation with $[L_b][C_b]^T$ yields the following relationship between the nodal forces and nodal displacements

$$\{F_b) = \rho_s\omega^2[L_b][C_b]^T[D'])[C_b]\{U_b\} \tag{26}$$

Let

$$[K_b] = \rho_s\omega^2[L_b][C_b]^T[D'][C_b] \tag{27}$$

Then Eq. (26) can be simplified to express the equilibrium equation for the fluid in terms of nodal displacements and forces, that is

$$\{F_b\} = [K_b]\{U_b\} \tag{28}$$

BEM formulation for the soil

The governing equation for soil layers that are homogeneous, isotropic, and linearly elastic with small displacements is the well known Navier equation. Expressed in terms of transformed displacements U in the frequency domain, Navier's equation is given by Eq. (29) where, for simplicity, zero initial conditions have been assumed; $k = i\omega$, and c_1 and c_2 are the P- and S-wave velocities, respectively [39]

$$(c_1^2 - c_2^2)U_{i,ij} + c_2^2U_{j,ii} - k^2U_j = 0 \tag{29}$$

The corresponding boundary conditions to Eq. (29) are

$$U_i(\vec{x}; k) = F_i(\vec{x}k) \qquad \vec{x} \in \Gamma_1 \tag{30}$$

$$T_i(\vec{x}; k) = G_i(\vec{x}; k) \qquad \vec{x} \in \Gamma_2$$

where $F(\vec{x}, k)$ and $G(\vec{x}, k)$ are known displacements and tractions at the boundaries Γ_1 and Γ_2.

The BEM is employed to numerically solve Eq. (29) together with the boundary conditions expressed by Eq. (30). Similarly to Eq. (4), the starting expression for the BEM is the boundary integral equation

$$\delta(\vec{\xi})U_i(\vec{\xi}, k) + \int_\Gamma T_{ij}^* d\Gamma = \int_\Gamma U_{ij}^* T_j d\Gamma \tag{31}$$

where the fundamental solutions: U_{ij}^*, T_{ij}^* are given by [34,38]

$$\begin{aligned} U_{ij}^*(\vec{\xi}, \vec{x}, k) &= \frac{1}{2\pi\rho c_2^2}(\Psi\delta_{ij} - \chi r, ir, j)T_{ij}^*(\vec{\xi}, \vec{x}, k) \\ &= \frac{1}{2\pi}\left[\left(\frac{d\Psi}{dr} - \frac{\chi}{r}\right)\left(\delta_{ij}\frac{\partial r}{\partial n} + r_{,j}n_i - 2\frac{\chi}{r}\right)n_j r_{,i}\right. \\ &\quad - 2r_{,i}r_{,j}\frac{\partial r}{\partial n} - 2\frac{d\chi}{dr}r_{,i}r_{,j}\frac{\partial r}{\partial n} + \left(\frac{c_1^2}{c_2^2} - 2\right) \\ &\quad \left.\times\left(\frac{d\Psi}{dr} - \frac{d\chi}{dr} - \frac{\chi}{r}\right)r_{,i}n_{,j}\right] \end{aligned} \tag{32}$$

where

$$\Psi = K_0\left(\frac{kr}{c_2}\right) + \frac{c_2}{kr}\left[K_1\left(\frac{kr}{c_2}\right) - \frac{c_2}{c_1}K_1\left(\frac{kr}{c_1}\right)\right] \tag{33}$$

$$\chi = K_2\left(\frac{kr}{c_2}\right) - \frac{c_2^2}{c_1^2}K_2\left(\frac{kr}{c_1}\right)$$

in which K_0, K_1 and K_2 are modified Bessel functions of the second kind and order 0, 1, and 2, respectively.

Following well established discretization procedures for the boundaries and using constant boundary elements, see Fig. 2(a), Eq. (31) leads to a set of $2N$ linear equations that relate the displacements to tractions, that is

$$[H]\{U^i\} = [G]\{T^i\} \tag{34}$$

where $[H]$ and $[G]$ are $2N \times 2N$ matrices, the $2N$ vectors $\{U^i\}$ and $\{T^i\}$ are the displacement and traction vectors on the boundaries for the ith layer, and N is the number of boundary elements. A description of the methodology is given in several references, e.g. [36,37].

In order to derive the equilibrium equation for the whole system, the traction vector $\{T^i\}$ in Eq. (34) must be replaced by a nodal force vector. Specifically, Eq. (34) can be cast into the following form after some simple matrix manipulations:

$$[K^i]\{U^i\} = \{F^i\} \tag{35}$$

where

$$[K^i] = [L][G]^{-1}[H] \tag{36}$$

$$\{F^i\} = [L]\{T^i\} \tag{37}$$

in which

$$[L] = \mathrm{diag}\{l_1 l_1 l_2 l_2 \cdots l_N l_N\} \tag{38}$$

where l_i is the length of the ith boundary element.

4. FEM formulation for the lock and coupling of BEM with FEM

4.1. FEM formulation for the lock

The Mindlin–Kirchhorff plate theory [40,41] is utilized in the FEM formulation for the lock. According to this theory, the governing equations for bending and axial deformation are uncoupled. For a 2-D problem in the frequency domain, the governing equation for bending is reduced to the Bernoulli–Euler beam equation

$$\frac{\mathrm{d}^4 U_y}{\mathrm{d}y^4} - \lambda_1^4 U_y = 0 \tag{39}$$

where

$$\lambda_1^4 = \frac{\rho_f h \omega^2}{D_\mathrm{f}} \tag{40}$$

in which D_f is the flexural rigidity of the plate defined by

$$D_\mathrm{f} = \frac{E_\mathrm{f} h^3}{12(1 - \nu_\mathrm{f}^2)} \tag{41}$$

where h represents the thickness of the plate, and ρ_f, E_f, ν_f are the modulus of elasticity, mass density, and Poisson's ratio of the plate, respectively. Notice that the bending stiffness EI in the classic Bernoilli–Euler beam theory for bending has been replaced by D_f to account for the longitudinal stiffness of the plate. The governing equation for axial deformation is given by

$$\frac{\mathrm{d}^2 U_x}{\mathrm{d}x^2} + \lambda_2^2 U_x = 0 \tag{42}$$

where

$$\lambda_2^2 = \frac{\rho_f \omega^2}{E_f/(1 - \nu_f^2)} \tag{43}$$

The lock is divided into m elements, see Fig. 2(a). Following standard FEM procedures, the equilibrium equations for the axial and flexural response in the frequency domain can be written in the form [42,43]

$$\begin{bmatrix} D_{uu} & D_{u\theta} \\ D_{\theta u} & D_{\theta\theta} \end{bmatrix} \begin{Bmatrix} U^\mathrm{f} \\ \theta \end{Bmatrix} = \begin{Bmatrix} F^\mathrm{f} \\ M \end{Bmatrix} \tag{44}$$

where the subscripts u and θ refer to nodal displacements and rotations, respectively and M denotes moments acting at the nodes. Through condensation of the rotational degrees-of-freedom, Eq. (44) can be rewritten in the following form [43]

$$\{F^\mathrm{f}\} = [K^\mathrm{f}]\{U^\mathrm{f}\} \tag{45}$$

where

$$[K^\mathrm{f}] = [D_{uu}] - [D_{u\theta}][D_{\theta\theta}]^{-1}[D_{\theta u}] \tag{46}$$

4.2. Coupling of BEM with FEM

The governing equation for the whole system can be obtained by enforcing compatibility and equilibrium conditions at the soil–structure and structure–fluid interfaces. Specifically, at the interfaces the displacements from each substructure should satisfy the relationships

$$\begin{aligned} \{U_\mathrm{e}\} &= \{U_\mathrm{e}^0\} \\ \{U_\mathrm{c}\} &= \{U_\mathrm{c}^0\} = \{U_\mathrm{c}^\mathrm{s}\} \\ \{U_\mathrm{b}\} &= \{U_\mathrm{b}^0\} = \{U_\mathrm{b}^\mathrm{a}\} = \{U_\mathrm{b}^\mathrm{f}\} \\ \{U_i\} &= \{U_i^{i-1}\} = \{U_i^i\} \\ \{U_\mathrm{g}\} &= \{U_n^n\} \end{aligned} \tag{47}$$

where the superscript s represents walls of the lock, f denotes fluid, and other superscripts indicate the location of a soil layer, subscripts denote the boundaries according to the adopted notation given earlier. The common displacements at the interfaces are indicated without superscripts, and U_g is the seismic excitation at the interface of the bedrock, see Fig. 1.

The forces from each substructure sum up to zero where no external forces are applied, that is

$$\begin{aligned} \{F_\mathrm{e}^0\} &= \{0\} \\ \{F_\mathrm{e}^0\} + \{F_\mathrm{c}^\mathrm{s}\} &= \{0\} \\ \{F_\mathrm{b}^0\} + \{F_\mathrm{b}^\mathrm{a}\} + \{F_\mathrm{b}^\mathrm{f}\} &= \{0\} \\ \{F_i^{i-1}\} + \{F_i^i\} &= \{0\} \end{aligned} \tag{48}$$

Combining the equilibrium equations for each substructure and employing the compatibility conditions at the interfaces, the equilibrium equation for a system is obtained [37]

$$[K]\{U\} = \{P\} \tag{49}$$

where

$$\{U\} = \{U_\mathrm{e}, U_\mathrm{c}, U_\mathrm{b}, U_1, \ldots, U_i, \ldots, U_{n-1}\}^T \tag{50}$$

$$\{F\} = \{0, 0, 0, 0, \ldots, 0, \ldots, -K_{n-1,n}^n\}^T U_\mathrm{g} \tag{51}$$

and

$$[K] = \begin{bmatrix} K_{ee}^0 & K_{ec}^0 & K_{eb}^0 & K_{e1}^0 & & & & & \\ K_{ce}^0 & K_{cc}^0 + K_{cc}^s & K_{cb}^0 + K_{cb}^s & K_{c1}^0 & & & & & \\ K_{be}^0 & K_{bc}^0 + K_{bc}^s & K_{bb}^0 + K_{bb}^s + K_{bb}^f & K_{b1}^0 & & & & & \\ K_{1e}^0 & K_{1c}^0 & K_{1b}^0 & K_{11}^0 + K_{11}^1 + K_{12}^1 & \cdots & & & & \\ & & & K_{21}^1 & & \cdots & K_{i-1,i}^{i-1} & & \\ & & & & & K_{i,i-1} & K_{i,i}^{i-1} + K_{i,i}^i & K_{i,i+1} i & \\ & & & & & & K_{i+1,i}^i & \cdots & \\ & & & & & & & \cdots & K_{n-2,n-1}^{n-1} \\ & & & & & & & K_{n-1,n-2}^{n-1} & K_{n-1,n-2}^n \end{bmatrix} \quad (52)$$

5. Numerical example and parametric studies

The soil–structure system consists of a lock with a width $2B$ embedded in a soil layer with a depth H over a half-space bedrock (see Fig. 2(b)). The discretization of the three domains, i.e. water, lock and soil are shown in Fig. 2(a). The depth of the embedment is D, and it is assumed that the fluid fills up the lock. In the numerical examples, the contained fluid is water. The material properties of the lock are: mass density $\rho_f = 2500\ \text{kg/m}^3$, Poisson's ratio $v_f = 0.3$, and damping ratio $\xi_f = 0.05$. The material properties of the soil are: modulus of elasticity $E_s = 100$ MPa, mass density $\rho_s = 2000\ \text{kg/m}^3$, Poisson's ratio $v_s = 0.33$, and damping ratio $\xi_s = 0.05$. To evaluate the effect of lock stiffness on the response, two cases, i.e. $E_f = 1 \times 10^3$ MPa and $E_f = 1 \times 10^6$ MPa are considered. Their relative stiffness is equal to 45 and 0.045, respectively. The relative stiffness and mass are defined by [44,45]

$$K_r = \frac{E_f h^3}{1 - v_f^2} \Big/ \frac{E_s B^3}{1 + v_s}, \qquad M_r = \frac{\rho_f}{\rho_s} \quad (53)$$

Locks with relative stiffness of 500, 5, and 0.05 are characterized as rigid, intermediate, and very soft, respectively. Thus, locks with relative stiffness of $K_f = 45$ and 0.045 can be considered as stiff and soft, respectively. The ratio of lock width to thickness of the soil layer is $H/B = 2$. Two different embedment depths to width ratios $D/B = 1$ and $D/B = 2$, are considered to investigate the effects of embedment on the response. A horizontal harmonic excitation with amplitude U_g and circular frequency ω is prescribed at the interface of the bedrock with the soil layer.

The results are presented in the form of relative displacements U_r, that is

$$U_r = \frac{U}{U_g} \quad (54)$$

where U is the displacement at either the structure surface or the top free surface.

Two factors of great importance in the BEM formulation using fundamental solutions of the infinite soil domain are the truncation distance L and the element size of the boundary elements l_l, see Fig. 2(b). To select optimum truncation distances and size of the boundary elements that maintain the balance between accuracy and efficiency for flexible foundations, a series of convergence studies has been conducted. For a detailed discussion, the reader is referred to the work by Xu [37]. The investigation in Ref. [37] arrived at the following general discretization guidelines for SSI analysis of systems subjected to seismic waves: the displacement response of the system can be divided into two different ranges, covering low and high frequency ranges with the fundamental frequency as the threshold. When the excitation frequencies are greater than the fundamental frequency, a sinusoidal-like curve that is referred to as 'standing wave' in the later discussion forms at the top free surface and vanishes after several circles. The convergence studies indicate that the required truncation distances should include four circles of standing waves, while the boundary element size should be one-tenth of the length of the standing wave. At the low frequency range, i.e. excitation frequencies lower than the fundamental frequency, the effect of discretization mesh is not so significant and larger element sizes as well as short truncation distances can be used.

Fig. 3(a)–(d) shows the relative displacements U_r at the center of the bottom side of the locks versus the nondimensionless frequency, A_0, defined by

$$A_0 = \frac{B\omega}{C_2} \quad (55)$$

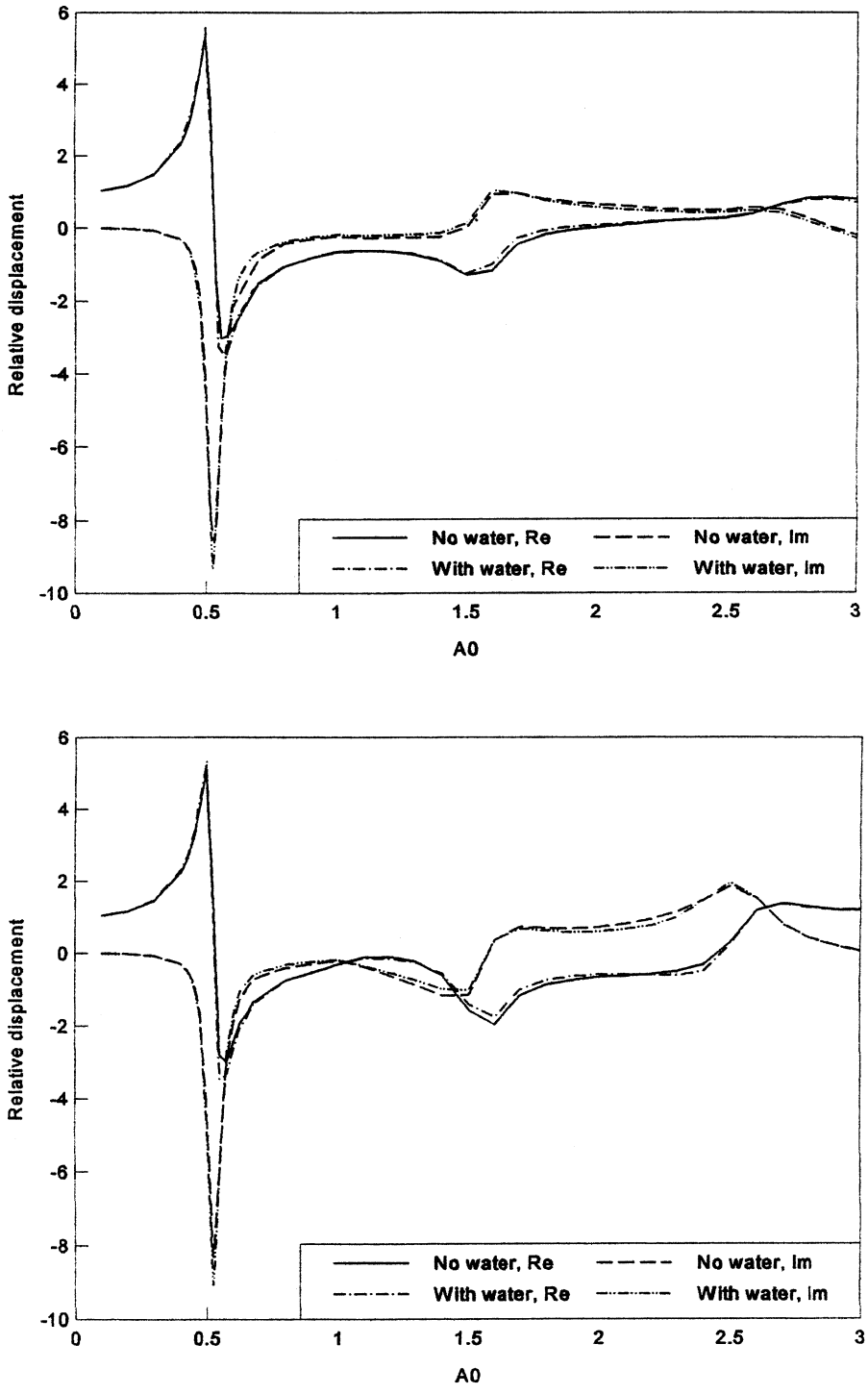

Fig. 3. Effect of water on relative displacement, U_r: (a) stiff foundation, $D/B = 1$; (b) soft foundation, $D/B = 1$; (c) stiff foundation, $D/B = 2$; (d) soft foundation, $D/B = 2$.

As indicated in Fig. 3, solid lines represent relative displacements when no water is present, while dash-lines indicate relative displacement when the water is included. It is observed that the effect of water on the seismic response is not significant, especially at the low frequency range, see Fig. 3(a)–(c). However, as shown in Fig. 3(d), the relative displacements are considerably affected by the presence of water at the high frequency range for a flexible lock with $D/B = 2$. Also note that at a frequency equal to the fundamental frequency of the system, the displacements for all the four cases with water present are different from those with no water present. Specifically, the displacements with water in the lock are larger than those without the presence of water.

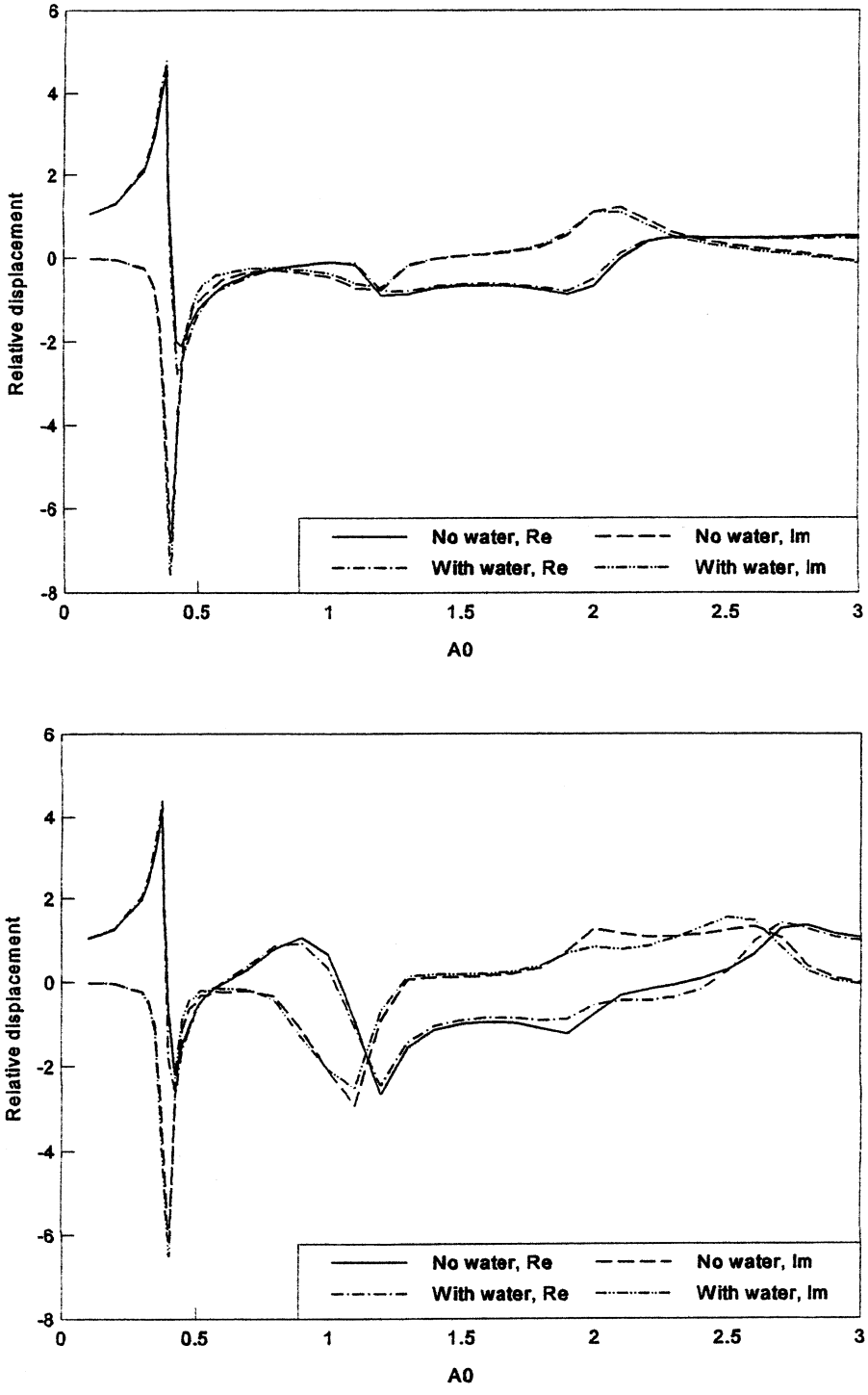

Fig. 3. (*continued*)

The effect of relative stiffness can be evaluated from Fig. 4(a) and (b) that shows the relative displacements U_r at the center of the bottom side of water-filled locks. Fig. 4(a) shows the displacements U_r for $D/B = 1$, and Fig. 4(b) depicts the displacements U_r for $D/B = 2$. Comparison between Fig. 4(a) and (b) clearly demonstrates that the effect of lock stiffness is significant. Although at low frequencies, i.e. A_0 less than the fundamental frequency, both soft and stiff locks respond similarly, at high frequencies soft locks react very differently from stiff locks. Also, notice that within a certain frequency range, the relative displacements for soft locks are much larger than those for stiff locks, while at some other frequency range, the reverse is observed. Therefore, the presence of the water

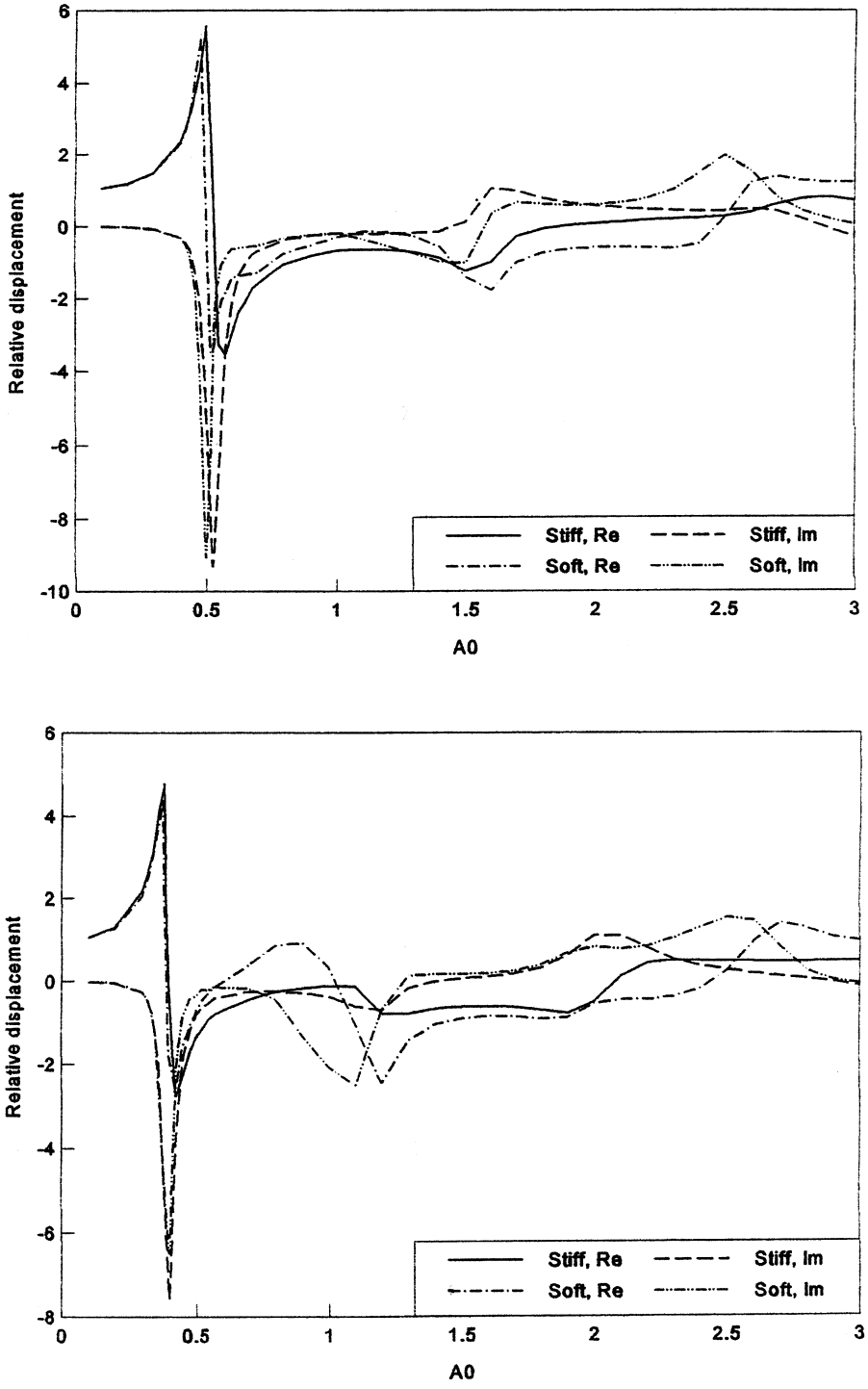

Fig. 4. (a) Effect of water foundation stiffness on relative displacement, U_r, ($D/B = 2$).

does not always have a beneficial effect on the system response. When Fig. 4(a) is compared to Fig. 4(b), larger differences on the response are observed for the lock with deeper embedment. Therefore, it is reasonable to conclude that the effect of lock stiffness becomes more significant when the embedment of the lock increases.

The effect of embedment on the response of the fluid filled locks is investigated next. Fig. 5(a) and (b) show the relative displacements at the center of the bottom side of a soft lock and a stiff lock, respectively, for $D/B = 1$ and $D/B = 2$. As shown in Fig. 5, for both stiff and soft locks, an increase of embedment causes a decrease of the fundamental frequency of the system. It is also observed that an increase of embedment reduces the displacements around the fundamental frequency, but may result in larger displacements at a higher frequency. Finally, comparison between

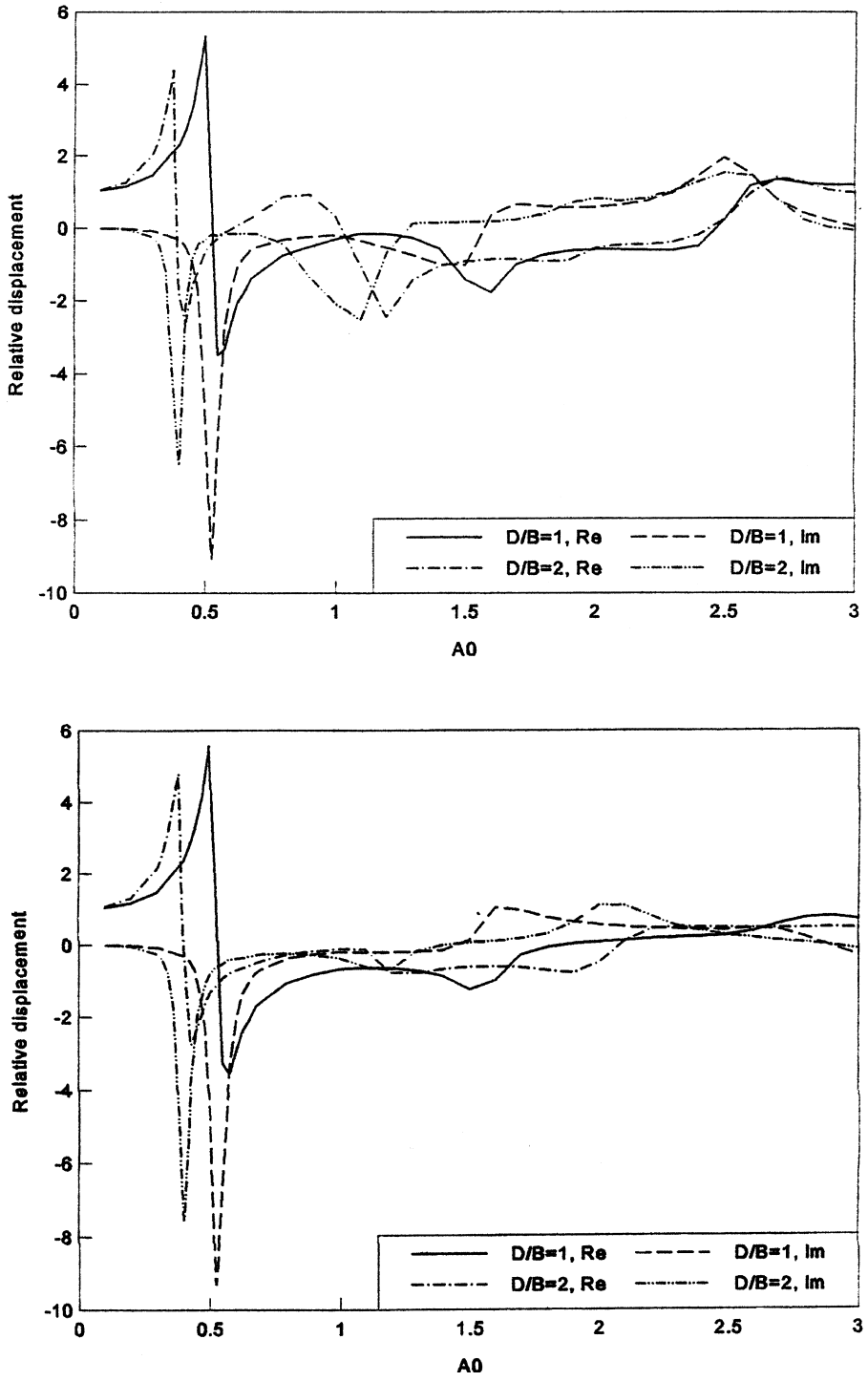

Fig. 5. Effect of foundation embedment on relative displacement, U_r: (a) soft foundation; (b) stiff foundation.

Fig. 5(a) and (b) shows that the effect of lock embedment is more significant for soft locks than for stiff locks.

6. Conclusions

A study has been presented on the soil–structure–fluid interaction analysis of a lock system subjected to harmonic seismic waves. The water contained lock is embedded in soil layers supported by a half-space bedrock. The ground excitation is prescribed at the soil–bedrock interface. Through a hybrid BEM–FEM formulation, the flexible lock is modeled by the FEM, while the semi-infinite soil layers and the contained

fluid are modeled by the BEM. The equilibrium equation of the system is assembled by enforcing compatibility and equilibrium conditions at the fluid–structure, structure–soil, and soil–layer interfaces.

The study demonstrates the important role the relative stiffness and embedment play on the seismic response of lock systems. Parametric studies are conducted to investigate the effects of hydrodynamic forces, the relative stiffness of the lock lining–soil system, and the embedment of the lock on the response. The study also shows that the fluid plays a significant role on the displacement amplitude of locks with small stiffness and large embedment. For other cases, however, the effect of fluid on the displacements could be omitted from the analysis, except for frequencies close to the fundamental frequency of the system. Specifically, when the frequency of the excitation is close to the fundamental frequency of the system, the displacements of a water-filled lock are much greater than those with no water present. The parametric studies demonstrate that an increase of either the relative stiffness or the embedment of the system does not warrant reduction of the system response for the same excitation.

References

[1] Chen LH. Acoustic emissions from submerged structures. In: Banerjee PK, Shaw RP, editors. Developments in boundary element methods—2. London: Applied Science, 1982. p. 245–81.

[2] Everstine GC, Henderson FM. Coupled finite element/boundary element approach for fluid–structure interaction. J Acoust Soc Am 1990;87(5):1938–47.

[3] Jeans RA, Mathews IC. Solution of fluid–structure interaction problems using a coupled finite element and variational boundary element technique. J Acoust Soc Am 1990;88(5):2459–66.

[4] Dominguez J, Medina F, Maeso O. Dynamic analysis of dam–soil–reservoir systems. In: Dominguez J, editor. Boundary elements in dynamics, 1993. p. 607–47.

[5] Hall JF, Chopra AK. Two-dimensional dynamic analysis of concrete gravity and embarkment dams including hydrodynamic effects. Earthquake Engng Struct Dyn 1982;10:305–32.

[6] Chavez JW. Earthquake response of concrete gravity dams including base sliding. ASCE J Struct Engng 1995;121(5):865–75.

[7] Antes H, Von Estorff O. Analysis of absorbtion effects on the dynamic response of dam reservoir systems by element methods. Earthquake Engng Struct Dyn 1987;15:1023–36.

[8] Fok K, Chopra AK. Water compressibility in earthquake response of arch dams. J Struct Engng 1987;113:958–75.

[9] Dominguez J, Medina F. Boundary elements for the analysis of the seismic response of dams including dam–water–foundation interaction effects. II. Engng Anal 1989;6:158–63.

[10] Jablonsky AM, Humar JL. Three-dimensional boundary element reservoir model for seismic analysis of arch and gravity dams. Earthquake Engng Struct Dyn 1990;19:359–76.

[11] Camara RJ. A method for coupled arch dam–foundation–reservoir seismic behavior analysis. Earthquake Engng Struct Dyn 2000;29(4):411–60.

[12] Antes H, Latz K. Soil–structure–fluid interaction. In: Manolis GD, Davies TD, editors. Boundary element techniques in geomechanics. New York: Elsevier Applied Science, 1993. p. 407–42.

[13] Housner GW. Dynamic pressure on accelerated fluid containers. Bull Seismological Soc Am 1957;47:15–35.

[14] Westergaard HM. Water pressures on dams during earthquakes. Trans ASCE 1933;98(11):413–8.

[15] Liaw C-Y, Chopra AK. Dynamics of towers surrounded by water. Earthquake Engng Struct Dyn 1974;3:33–49.

[16] Veletsos A, Yang JY. Dynamics of fixed-base liquid storage tanks. Earthquake Engng Struct Dyn 1976;7:587–601.

[17] Haroun MA, Housner GW. Dynamic characteristics of liquid storage tanks. J Engng Mech ASCE 1982;108:783–800.

[18] Goyal A, Chopra AK. Hydrodynamic mass for intake towers. J Engng Mech ASCE 1989;115(7):1393–412.

[19] Haroun MA, Tayel MA. Axisymmetrical vibrations of tanks—analytical. J Engng Mech 1985;111:346–58.

[20] Veletsos AS, Tang Y. Dynamic response of vertically excited liquid tanks. J Struct Engng 1986;112:1228–46.

[21] Veletsos AS, Tang Y. Soil–structure interaction effects for laterally excited liquid storage tanks. Earthquake Engng Struct Dyn 1990;19:473–96.

[22] Fischer FD, Seeber R. Dynamic analysis of vertically excited liquid storge tanks considering liquid soil interaction. Earthquake Engng Struct Dyn 1988;16:329–42.

[23] Seeber R, Fischer FD, Rammerstorfer FG. Analysis of a three-dimensional tank–liquid–soil interaction problem. J Pressure Vessel Tech 1990;112:28–33.

[24] Spyrakos CC, Xu CJ. Soil–structure–water interaction of intake–outlet towers allowed to uplift. Soil Dyn Struct Engng 1997;16:151–7.

[25] Edwards NW. A procedure for dynamic analysis of liquid storage tanks subjected to lateral ground motion. PhD thesis. University of Michigan, Ann Arbor, 1969.

[26] Liu WK. Finite element procedures for fluid–structure interactions and application to liquid storage tanks. Nucl Engng Des 1981;65:211–38.

[27] Ma DC, Gvildys YW, Liu WK. Seismic behaviour of liquid-filled shells. Nucl Engng Des 1982;70:437–55.

[28] Balendra T, Ang KK, Paramasivam P, Lee SL. Seismic design of flexible cylindrical liquid storage tanks. Earthquake Engng Struct Dyn 1982;10:477–96.

[29] Barton DC, Parker JV. Finite element analysis of the seismic response of anchored and unanchored liquid storage tanks. Earthquake Engng Struct Dyn 1987;15:299–322.

[30] Kumastu K. Fluid structure interaction. In: Brebbia CA, editor. Progress in boundary element methods, vol. 2. London: Pentech, 1981. p. 182–99.

[31] Walker S. Boundary elements in fluid–structure interaction problems rotational shells. Appl Math Modelling 1980;4:345–50.

[32] Koh HM, Kim JK, Park JH. Fluid–structure interaction analysis of 3-D rectangular tanks by a variationally coupled BEM–FEM and comparison with test results. Earthquake Engng Struct Dyn 1998;27:109–24.

[33] Park J-H, Koh HM, Kim J. Fluid–structure interaction analysis by a coupled boundary element–finite element method in time domain. In: Brebbia CA, editor. Boundary element technology VII, London: Elsevier, 1992. p. 227–43.

[34] Spyrakos CC. Strip-foundations. In: Manolis GD, Davies TD, editors. Boundary element techniques in geomechanics. New York: Elsevier Applied Science, 1993.

[35] Bachelor GK. An introduction to fluid mechanics. Cambridge: Cambridge University Press, 1967.

[36] Dominguez J. Boundary elements in dynamics. New York: Elsevier Applied Science, 1993.

[37] Xu CJ. Dynamic soil–structure interaction by hybrid FEM–BEM. PhD dissertation. Morgantown, WV: West Virginia University, 1995.

[38] Cruse TV, Rizzo FJ. A direct formulation and numerical solution of the general transient elasto-dynamic problem. J Math Anal Appl 1968;22:244–59.

[39] Wolf PJ. Dynamic soil–structure interaction. New York: Prentice-Hall, 1994.

[40] Timosheko SP, Woinowsky-Krieger S. Theory of plates and shells. New York: McGraw-Hill, 1959.
[41] Ugural AC. Stresses in plates and shells. New York: McGraw-Hill, 1981.
[42] Paz M. Structural dynamics: theory and computation. 3rd ed. Van Nostrand Reinhold Company, 1991.
[43] Spyrakos CC. Finite element modeling in engineering practice. Algor Publishing Division: Pittsburgh, PA, 1995.
[44] Kokkinos FT, Spyrakos CC. Dynamic analysis of flexible strip-foundations in the frequency domain. Computers & Structures 1991;39(5):473–82.
[45] Antes H, Spyrakos CC. Soil–structure interaction. In: Beskos DE, Anagnostopoulos SA, editors. Computer analysis and design of earthquake resistant structures: a handbook. Boston, MA: Computational Mechanics Publications, 1997.